

# OPTIMAL DESIGN OF A MULTIMODAL DYNAMIC VIBRATION ABSORBER IN THE PRESENCE OF UNCERTAINTIES

**Murilo Borges Barros, murilobbarros@gmail.com**

**Domingos Alves Rade, domingos@ufu.br**

**Ricardo Gonçalves de Sales, rgs\_mecanica@yahoo.com.br**

**Emmanuel Pillet, manu.pillet@gmail.com**

Federal University of Uberlândia - School of Mechanical Engineering, Campus Santa Mônica, 38400-902, Uberlândia - MG, Brazil

**Edmar Baars, edmar.baars@embraco.com.br**

Whirlpool-EMBRACO S.A., Rua Rui Barbosa, 1020, 89219-901, Joinville - SC, Brazil

***Abstract.** Dynamic Vibration Absorbers (DVA) are widely used for passive control of structural vibrations. In their simplest configurations, those devices have their mitigation capacity confined to narrow frequency bands, which limits, to a large extent, their practical effectiveness. In this work, it is proposed a methodology for the optimal design of a multimodal dynamic vibration absorber, intended to attenuate the amplitude levels around various resonant peaks simultaneously. The optimization is done taking account design constraints. Moreover, the variability inherent to the construction of the base structure and of the DVA itself is considered aiming at obtaining robust designs. To evaluate the dynamic response of the dynamical system, a technique for substructure coupling based on frequency response functions (FRFs) is used to evaluate the dynamic behavior of the coupled structure (base structure + DVA), given the FRFs of each substructure separately. Monte Carlo simulation is used to evaluate the influence of the uncertainties on the effectiveness of the multimodal DVA. The procedure is illustrated by numerical and experimental results obtained for an industrial structure.*

***Keywords:** dynamic vibration absorbers; robust design; uncertainty propagation*

## 1. INTRODUCTION

In scope of mechanical engineering, vibration control must be considered in many circumstances. To control undesirable vibrations, two broad categories of methods are considered: active methods and passive methods. The present work focuses on the use of dynamic vibration absorbers (DVAs) which are passive devices.

Basically, a DVA is a mass-string-damper oscillator. When connected to a primary mechanical system whose vibration level must be attenuated, a DVA is able to capture and possibly dissipate part of the vibration energy of this system, thus reducing the vibration amplitudes at the connection between the DVA and the primary system. Since its invention by Frahm in the beginning of the 20<sup>th</sup> century (Frahm, 1911), this basic type of DVA and other more involved configurations (such as those represented by multi-degree-of-freedom systems (Ram and Elhay, 1996) and continuous system (Snowdon and Nobile, 1980) been extensively applied to various type of machines and structures, in different branches of the industrial activity.

Traditionally, the DVA parameters (mass, stiffness and damping) are chosen – and the DVA is said to be tuned - to minimize vibrations generated by a harmonic excitation in the vicinity a given value of the excitation frequency. However, the absorber tends to lose efficiency if the frequency of excitation, or one or more constructive parameters of the DVA, change, even slightly. In such cased the DVA becomes mistuned and it is possible that vibration levels increase with respect to the baseline condition. To circumvent this problem, a feasible strategy consists in determining a set of parameters guaranteeing minimum amplitude of vibration in the widest possible frequency range. This procedure is known as DVA optimization. From the pioneering works of Brock (1946) and Den Hartog (1956), various methods of optimization were proposed, based either in the time or frequency domain responses (Rade and Steffen, 1999).

Another aspect which is becoming increasingly incorporated in structural dynamic analysis is uncertainty propagation, which encompasses a number of numerical techniques intended to evaluate the influence of modeling or experimental uncertainties on the dynamic responses of mechanical systems (Adhikari 2009, Sudret 2007, Worden 2005; Schüeller, 1997). Such problem is particularly relevant in the design of vibration control devices as the attenuation performance can be strongly influenced by the presence of uncertainties. This fact leads to the necessity of designing control systems which are as robust as possible with respect variations of their design parameters and operational conditions.

In this context, the purpose of this paper is to present a general methodology used for the optimal design of a multimodal dynamic vibration absorbers (MDVA), which has been conceived to attenuate vibrations in the vicinity of an arbitrary number of target frequencies.

## 2. THEORETICAL FOUNDATIONS

The following developments are based on Den Hartog (1956) and Dimaragonas (1996) works. Consider the system represented in Figure 1. We desire to attenuate the primary system vibrations by mean of a coupled DVA. It is admitted

that the primary system is excited by a harmonic force with amplitude  $F_0$  and frequency of excitation  $\Omega$ . This frequency of excitation has a fixed value that does not coincide necessarily with the natural frequency of the system.

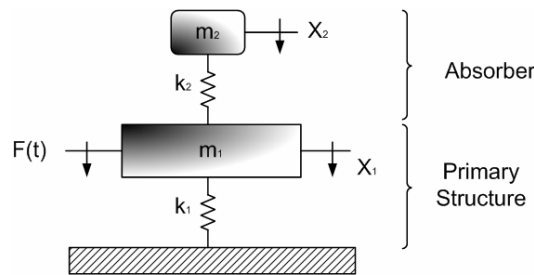


Figure 1 - Model of a primary structure with undamped dynamic absorber (Cunha Jr., 1999).

The steady-state amplitude  $X_1$  of the primary system is given by:

$$\frac{X_1}{F_0 k_1^{-1}} = \frac{\left[ 1 - \left( \frac{\Omega}{\omega_a} \right)^2 \right]}{\left[ 1 + \frac{k_2}{k_1} - \left( \frac{\Omega}{\omega_n} \right)^2 \right] \left[ 1 - \left( \frac{\Omega}{\omega_a} \right)^2 \right] - \frac{k_2}{k_1}} \quad (1)$$

where:

$$\omega_n = \sqrt{\frac{k_1}{m_1}} : \text{natural frequency of the primary system, considered alone} \quad (2.a)$$

$$\omega_a = \sqrt{\frac{k_2}{m_2}} : \text{natural frequency of the DVA, considered alone} \quad (2.b)$$

It can be observed in Eq. (1) that the response amplitude of the primary system vanishes when the numerator is zero, which occurs when the excitation frequency  $\Omega$  coincides with the natural frequency of the DVA,  $\omega_a$ . From the graphical representation of Eq. (1) in Figure 2, one can notice the typical FRF of a 2 degree-of-freedom system with two natural frequencies. The introduction of the DVA allows to generate an anti-resonance in the frequency response function (FRF) at  $\Omega = \omega_a$ .

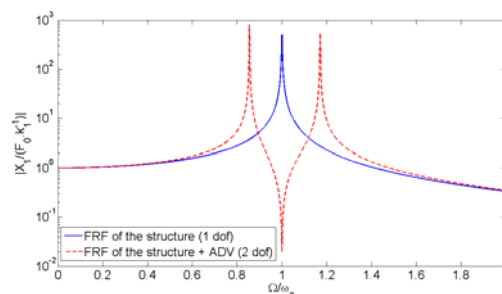


Figure 2 – FRF of the primary mass  $m_1$ , for  $m_2/m_1 = 0,20$ .

An optimal DVA design should preferably attain a maximum attenuation of vibrations in a relatively large frequency band centred on a nominal target frequency. This goal can be achieved with the introduction of an energy dissipation mechanism (damping) in the absorber. The damping also plays the important role of limiting the amplitude of vibration of the absorber itself, which allows satisfying design constraints related to fatigue endurance (Dimaragoras,

1996). Consider the system represented in Fig. 3, composed of a DVA with viscous damping ( $m_2, c_2, k_2$ ) attached to an undamped primary system ( $m_1, k_1$ ).

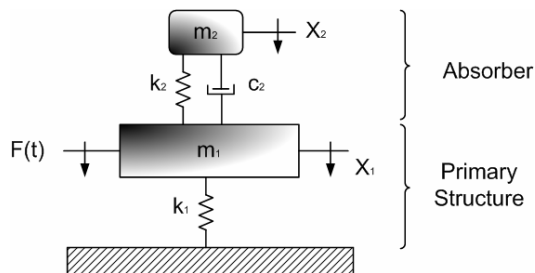


Figure 3 – Primary system with a DVA with viscous damping.

One can easily derive the following expression for the amplitude  $X_1$  of the primary system, in terms of dimensionless parameters:

$$\frac{|X_1|}{X_{est}} = \sqrt{\frac{(2\eta g)^2 + (g^2 - f^2)^2}{(2\eta g)^2 (g^2 - 1 + \mu g^2)^2 + [\mu f^2 g^2 - (g^2 - 1)(g^2 - f^2)]^2}} \quad (4)$$

where:

- $\mu = m_2/m_1$  : mass ratio;
- $\omega_a = \sqrt{(k_2/m_2)}$  : undamped natural frequency of the DVA (isolated);
- $\omega_n = \sqrt{(k_1/m_1)}$  : natural frequency of the primary structure, (isolated);
- $f = \omega_a/\omega_n$  : ratio of natural frequencies;
- $g = \Omega/\omega_n$  : ratio of forced frequencies;
- $c_c = 2m_2\omega_n$  : critical damping;
- $\eta = c/c_c$  : damping factor;
- $X_{est} = F_0/k_1$  : static deflection of the primary system.

Figure 4 depicts the plots of the dimensionless response amplitudes considering  $\mu = 1/20$  and  $f = 1$ , and different values of the damping factors. It becomes clear that the introduction of damping in the DVA leads to lower average vibration amplitudes in a wider frequency band around  $\Omega/\omega_n = 1$ , as compared to undamped DVAs. However, very high damping can cause the two masses be virtually linked so as to form a one-degree-of-freedom system with mass  $m_1 + m_2$ .

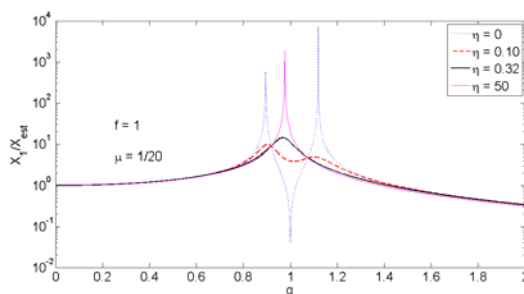


Figure 4 – Response amplitudes of the primary mass  $m_1$  for different values of the damping in the DVA.

As demonstrated in numerous studies (Cunha Jr., 1999), the theory presented above can be extended to the case in which the DVA is composed by a continuous structure. In this case, attenuation of the vibrations of the primary system can be achieved in the vicinity of each natural frequency of the DVA, with the point connected to the primary system grounded. This is the case considered in the present study. Figure 5 illustrates the DVA geometry, which is

resembles a flower, each petal of which is designed to behave like a cantilever beam with a concentrated mass at the free end. The design procedure consists in determining a set of geometrical parameter values in such a way the natural frequencies of the beams match the target frequencies.

### 2.1. Substructure coupling based on FRFs

The technique, originally proposed by Crowley et al. (1984) and Otte et al. (1991), was recently adapted by Rade and Steffen (1999) to the problem of optimization of DVAs parameters.

The main objective is to determine FRFs of the coupled system (primary system + DVAs), starting from FRFs of the primary system and FRFs of the DVAs. The FRFs of the coupled system can be then used in optimization procedures.

Let  $H_A$  be the driving point FRF of the primary system and  $H_B$  the FRF of the DVA, related to the connecting point of each substructure, the frequency response  $H_C$ , of the coupled system, at the coupling point, can be obtained from the following expression:

$$H_C = H_A (H_A + H_B)^{-1} H_B \quad (5)$$

It has been shown in previous studies that the use of such coupling technique is very advantageous in a number of circumstances, in particular because it enables to predict the dynamic behavior of the coupled system by mixing numerical and experimental data, as it has been done in this study reported herein.

### 2.2. Uncertainty propagation

When designing a mechanical system, we have to keep in mind that the inevitable presence of uncertainties are likely to affect different stages of analysis and design. Uncertainty is generally classified into two main categories, namely epistemic or reducible uncertainty, and random or irreducible uncertainty (Oberkampf, 2002). The first one is due to a lack of knowledge and takes place for instance in the choice of the constitutive laws. Random uncertainty, on the other hand, is inherent to the system and its operation environment. Mechanical properties, components assembly, manufacturing tolerances are subjected to this type of uncertainty. Mechanical systems which are little sensitive to those uncertainties are said to be robust.

An important step in the design of a robust system is the propagation of uncertainty through its numerical model. As the ultimate purpose of this study is to obtain robust DVAs, in this study Monte Carlo simulation is used to evaluate the influence of manufacturing uncertainties (especially tolerances), based on a simplified model of the DVA.

A model of uncertainty is needed to perform uncertainty propagating and, for this, various methods can be found in the literature. Probabilistic (Schuller, 1997), interval (Dessombz, 2001) or fuzzy (Massa, 2008) approaches are the most common representations used in mechanical engineering. In this paper, a classical probabilistic propagation is applied. Probability density functions (PDFs) are associated to some geometrical model parameters to represent tolerance uncertainty, a Latin Hypercube sampling (Helton 2003) is then carried-out to obtain input samples that are propagated through a finite element model. The lower and upper bounds of the driving point FRF related to the connection point between the primary system and the DVA are evaluated. The results are presented at the end of section 3.

## 3. METHODOLOGY

Initially, the DVA was modelled with plate elements. However, due to the high computational cost involved in the optimization using such a complex model, it was decided to replace the plate model with a model composed of three-dimensional beam and concentrated mass elements. The numerical model was modelled with the software ANSYS using elements SHELL63, for the plate model and BEAM4 and MASS21 for the equivalent beam model of beams. Figure 5 illustrates the two models used.

It should be noted that the model with shell elements is the real geometry of the DVA, to be used in its construction, while the simplified beam model is used in the optimization procedure.

The main advantage of working with beam models is a lower computational cost, since they generally have a smaller amount of degrees of freedom. Another relevant advantage is that an analytical expression of the first natural frequency of a clamped-free beam with concentrated mass in the free extremity is available in the literature (Blevins, 2001):

$$f = \frac{1}{2\pi} \sqrt{\frac{3EI}{l^3 (M + 0,24M_b)}} \quad (6)$$

where  $E$  is Young modulus,  $I$  the second moment of area of the beam cross section,  $l$  the length of the beam,  $M_b$  the total mass of the beam and  $M$  the concentrated mass

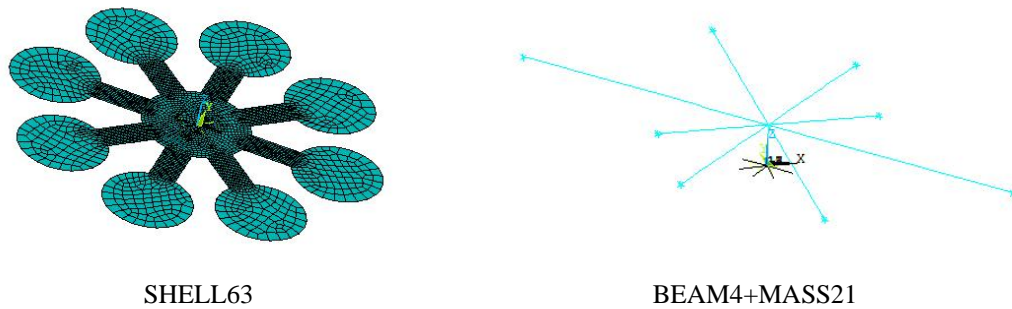


Figure 5 – Finite element model of the DVA.

Equations (7) establish the relations between the geometric characteristics used to generate the models based on shell (Fig. 6 (a)) and beam elements (Fig. 6 (b)).

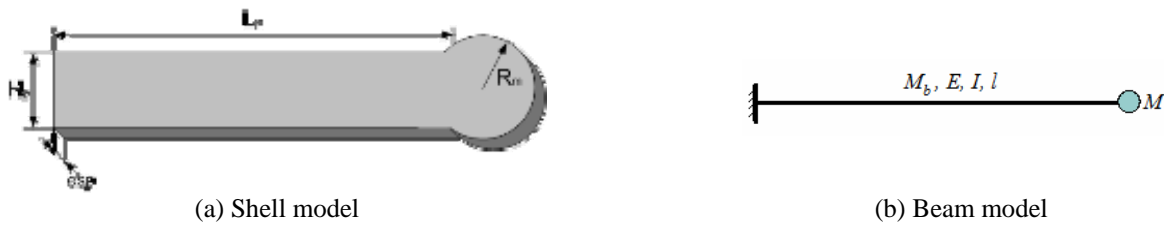


Figure 6 – Geometrical characteristics of the two models of DVA.

$$M_b = H_p \cdot \text{esp} \cdot L_p \cdot \rho \quad (\text{mass of the beam})$$

$$M = \pi \cdot R_m^2 \cdot \text{esp} \cdot \rho \quad (\text{concentrated mass at the free extremity}) \quad (7)$$

$$I = \frac{H_p \cdot \text{esp}^3}{12} \quad (\text{area moment of inertia of the beam})$$

Some numerical tests were performed to compare the eigenfrequency values obtained from each model. This comparison is shown in Table 1, revealing that the beam model provides eigenfrequencies very close to those obtained with the shell model, with an average deviation slightly larger than 1%. Thus, it can be concluded that the simplified model satisfactorily represents the dynamic behaviour of the DVA in the context of the considered project.

Table 1 – DVA natural frequencies obtained for the two types of models.

SHELL	301.68	1901.1	5348.8	10532	17494	26262	36869	49355	63773	80183	Mean
BEAM	286.18	1847.8	5271.7	10473	17482	26301	36925	49347	63558	79553	Deviation
Deviation (%)	5.14	2.80	1.44	0.56	0.07	0.15	0.15	0.02	0.34	0.79	1.10

Once validated the equivalent beam model, a procedure was carried-out aiming at optimizing the parameters of the DVA beams ( $H_p$ ,  $L_p$ ,  $R_m$ ) to attenuate a given number of resonance amplitudes of a flat plate, whose FE model is shown in Fig. 7a. The optimization procedure was adopted as follows:

- 1) Modeling of the plate using program ANSYS<sup>®</sup> and performing modal analysis to obtain the first four eigenfrequencies of the plate, which were considered as the target frequencies;
- 2) Performing harmonic analysis of the plate alone to obtain the FRFs in the frequency range including the target frequencies;
- 3) Determination of the optimal geometrical parameter values of the DVA using an optimization routine written in MATLAB<sup>®</sup>. Successively applied to each beam of the DVA, the objective function of the optimization procedure represents the absolute difference between the target frequency and the first eigenfrequency of beam. The optimization procedures implemented with the function *fmincon* of Matlab were used. The design variables

adopted are:  $L_p$ ,  $H_p$  and  $R_m$  (see Fig. 6a). The objective function and the constraint equations are given in Eq. (8) and (9), respectively.

$$f_{obj} = \min(|f_{plate} - f_{DVA}|) \quad (8)$$

$$0.015 \leq L_p \leq 0.060 \quad ; \quad 0.005 \leq H_p \leq 0.015 \quad ; \quad 0.6H_p \leq R_m \leq 2H_p \quad (9)$$

- 4) Coupling of the optimized DVA to the center of the plate and performing new harmonic analysis to obtain the FRF of the plate+DVA aiming at evaluating the DVA's performance. Figure 7b shows the plate with the DVA attached to its center through a rigid rod.

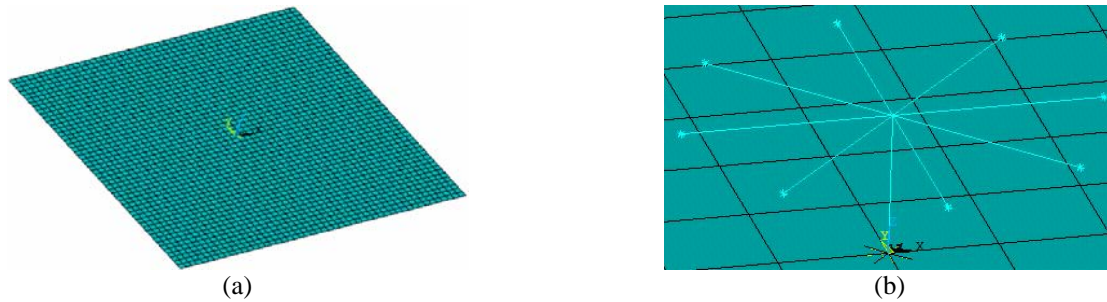


Figure 7 – a) Rectangular flat-plate model; b) Detail of the coupling plate-DVA.

Tables 2 and 3, respectively, show the values of the geometric properties of the base plate and the optimized DVA. For both the plate and the DVA, the used material is the steel. The thickness of the DVA is 1mm.

Table 2 – Base plate properties.

Width [m]	Length [m]	Thickness [m]
0.3	0.3	0.002

Table 3 – DVA properties.

Frequency (Hz)	Length $L_p$ [m]	Width $H_p$ [m]	Radius of the circle $R_m$ [m]	Equivalent concentrated mass $M_c$ [m]
198	0.0299	0.0120	0.024	0.0142
724	0.0211	0.0054	0.007	0.0012
1204	0.0172	0.0042	0.005	0.0006
1694	0.0134	0.0097	0.008	0.0016

It should be remembered that the DVA consists of pairs of symmetrical beams, the number of which correspond to the number of target natural frequencies. The set of design parameters is formed by the geometrical parameters of each individual pairs of beams.

Figure 8 compares FRFs of the plate before and after the coupling with the DVA at the connection point.

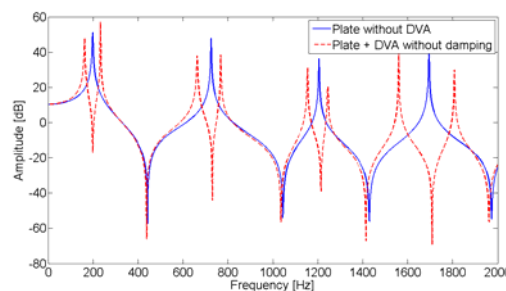


Figure 8 – Comparison of the plate FRFs with and without coupled DVA.  
 (note: amplitudes in dB with reference  $1.0 \times 10^{-6}$ )

One can verify that, upon introduction of the DVA, the FRF of the composite system plate-DVA has antiresonances in the values corresponding to the eigenfrequencies of the plate. However, there are also two new resonances in the neighbourhood of each frequency, which makes the DVA effective in very limited frequency band around the target frequencies. This situation can be avoided with the inclusion of damping in the DVA (Brock, 1946), making these two peaks to decrease dramatically or even disappear. To preliminarily evaluate this possibility, it was arbitrarily added to a 2% modal damping into the DVA model, providing the FRF shown in Fig. 9, which confirms that the inclusion of damping improves the effectiveness of the DVA in terms of amplitude reduction. A constant modal damping factor of 2% was arbitrarily chosen in order to account for inherent dissipation, which is a value typically found in assembled structural systems.

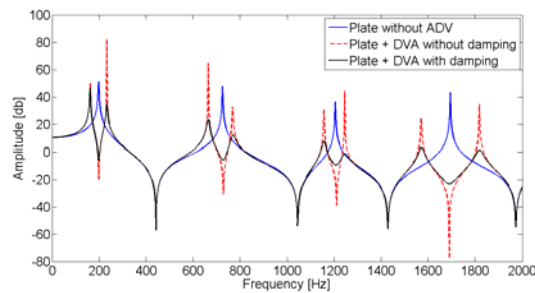


Figure 9 – FRF of the plate+DVA with and without damping.

To account for manufacturing uncertainties (dimensional tolerances), the dimensions  $L_p$ ,  $H_p$  and  $R_m$  are assumed to be subjected to random variability. No study was conducted with experimental DVA prototypes to determine the most adapted PDF associated with this dimensional uncertainty. As our knowledge about the uncertainty is minimum, for each parameter, we chose to a priori represent the uncertainty with a uniform PDF of relative small dispersion. Let  $p^{(0)}$  be the nominal value of a parameter, then the lower and upper bound of the uniform PDF are respectively  $0.95p^{(0)}$  and  $1.05p^{(0)}$ . The distribution is sampled by Latin Hypercube to obtain 1000 samples. The samples are propagated through the damped FE model (with 2% modal damping) and the driving point FRFs related to the connection point are calculated. In Figure 10 are plotted the FRF amplitudes for the plate without DVA (dashed line), for the plate with the nominal optimal DVA (centred thick line) and the envelopes of the FRF samples which delimit an uncertainty zone coloured in grey. It can be noticed that the uncertainty zone does not cover the first and fourth peaks of the FRF but covers the second and the third. This covering indicates that those resonances might not be satisfactorily attenuated for some parameter values resulting from tolerance uncertainties. Based on those visual considerations, one can conclude that the coupled system is more robust with respect to parameter uncertainties for the first and fourth modes than it is for the second and the third modes. As the DVA fails to attenuate in a robust manner some target frequencies, a robust optimization of the DVA becomes necessary. The robust optimization is not intended in this preliminarily study but robustness should be addressed in further developments.

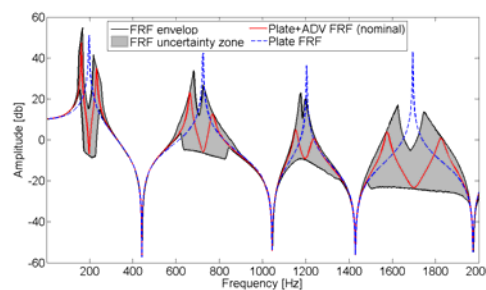


Figure 10 – FRF envelop of the coupled system after uncertainty propagation.

#### 4. APPLICATION TO AN INDUSTRIAL STRUCTURE

The procedure was tested upon application to a hermetic refrigerator compressor provided by EMBRACO. Experimental tests were carried-out with the following equipment: signal analyser Agilent model 35670A; impact hammer with load cell PCB model 086C01 with nominal sensitivity 11,2 mV/N; accelerometer PCB model 352C22 with nominal sensitivity 0,91 mV/ms<sup>-2</sup>; inertial table; cables and connections. The compressor was suspended through

flexible nylon strings so that free boundary conditions were obtained. The experimental assembly is shown schematically in Fig. 11(a) and 11(b).

Twenty two points were marked along the planes of symmetry of the compressor. The tests were performed by placing the accelerometer at one of these points and impacting with the modal hammer at the others. Figure 11(c) shows in detail the compressor with some of the test points.

As an example, Fig. 12 presents the amplitude, phase and coherence functions of the driving point FRF related to point 1 in the frequency band [2000 Hz ; 6400 Hz] with a step frequency of 4 Hz. A DVA was calculated to attenuate simultaneously four resonances, which were chosen arbitrarily in this frequency band. The optimization and the coupling of the optimized DVA were conducted according to the procedure described in Section 3. The target modes are those related in the following natural frequencies: 3160 Hz, 3404 Hz, 3684 Hz and 4824 Hz.

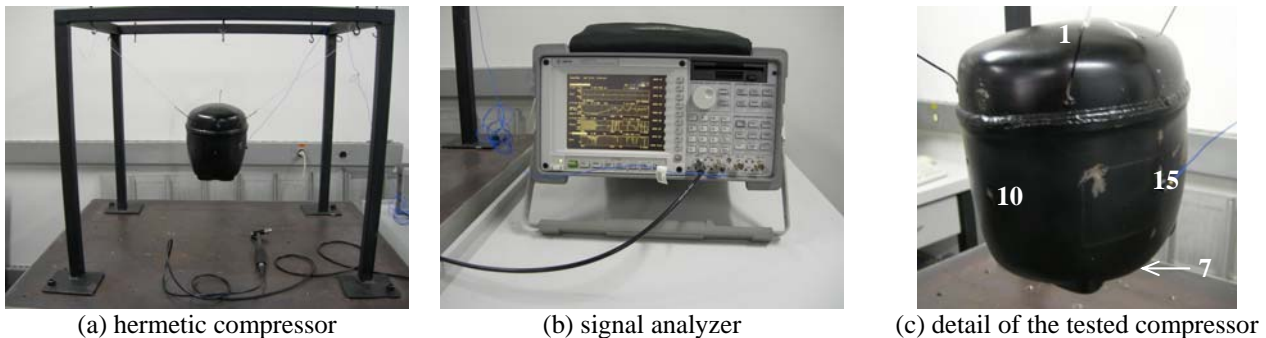


Figure 11 – Experimental bench.

After optimization, dimensions found were those shown in Table 4. The steel plate thickness of 0.001m was considered. The lateral constraints imposed to the optimization procedure were:

$$0.010 \leq L_p \leq 0.020 \quad , \quad 0.001 \leq H_p \leq L_p \quad , \quad 0.6H_p \leq R_m \leq 2H_p \quad , \quad M_c = \pi.R_m^2.esp.\rho$$

Table 4 – Optimal dimensions of the DVA.

Frequency (Hz)	Length $L_p$ (m)	Width $H_p$ (m)	Concentrated mass $M_c$ (kg)
3160	0.0090	0.0046	$7.474 \times 10^{-4}$
3404	0.0089	0.0048	$6.960 \times 10^{-4}$
3684	0.0083	0.0041	$6.318 \times 10^{-4}$
4824	0.0069	0.0048	$7.468 \times 10^{-4}$

With those dimensions, the DVA is simulated in ANSYS and harmonic analysis with modal superposition is performed to obtain the FRF of the DVA in the frequency band of interest. Figure 13 shows the FRF of the compressor and the DVA obtained in ANSYS. The target frequencies are 3160, 3404, 3684 and 4824 Hz.

Using the procedure described in Section 3, we can find the FRF of the coupled ensemble. The coupling was done for two different cases: DVA without damping and DVA with 2% of the modal damping. The FRF of the system compressor-DVA was computed by using the coupling procedure described in Section 2.1.

Figure 14 shows the comparison between the FRFs of the compressor without DVA and those of the combined structure compressor-DVA. It can be clearly perceived that the modes of interest were strongly attenuated, especially when damping is included in the DVA. As expected, it can be seen that the inclusion of the DVA entails the appearance of additional resonance peaks, inside and outside the target frequency band. However, in actual situations, such amplitude peaks can be attenuated by the introduction of additional damping, such as viscoelastic treatments.

As in section 3, parameter uncertainty is propagated through the coupled system. The lower and upper bounds of the used uniform PDFs are respectively  $0.98p^{(0)}$  and  $1.02p^{(0)}$ . Amplified pictures of the FRF around the target frequencies are presented in Fig. 15. It can be noticed that the system is robust to uncertainty for the second target frequency (3404 Hz) since the superior envelop of the uncertainty zone is of very low amplitude. The resonances of the first and two last target frequencies (3160 Hz, 3684 Hz and 4824 Hz) are not really covered by the uncertainty zone but for each one, appear peaks of high amplitude near the resonances to attenuate. Considering the magnitude of the uncertainty zone, the natural frequencies 3160 Hz, 3684 Hz and 4824 Hz are attenuated even with variability in the DVA parameters but the problem is shifted to neighborhood resonances. We consider the DVA really robust if no generated resonances exist. Clearly, this effect can be mitigated by increasing the DVA damping, whose level is limited by practical constraints. Nonetheless, the results demonstrate the interest and necessity of developing a robust optimization method for the DVA that will consider target frequencies but also neighborhood resonances induced by the DVA.



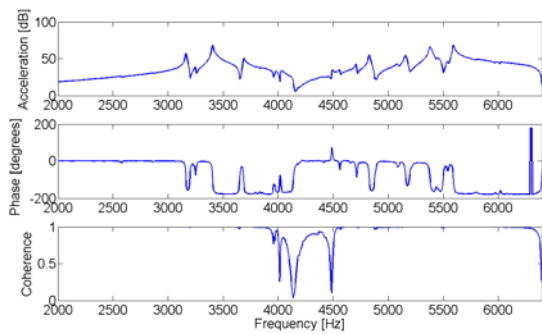


Figure 12 – Experimental FRF and coherence function

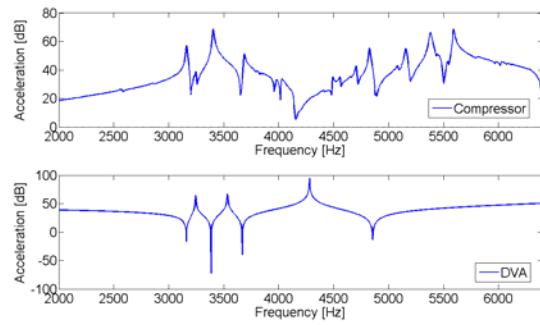


Figure 13 – Experimental FRF of the compressor alone and FE-computed FRF of the DVA.

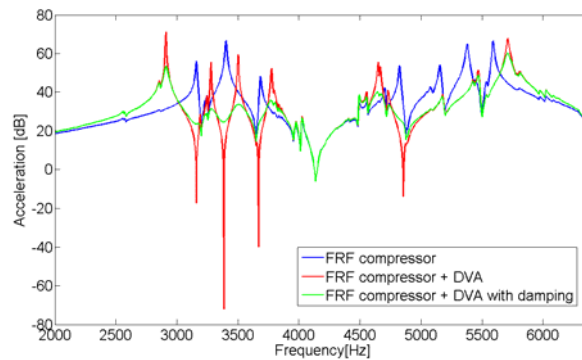


Figure 14 – Comparison of the FRF of the compressor with the FRFs of the system compressor-DVA.

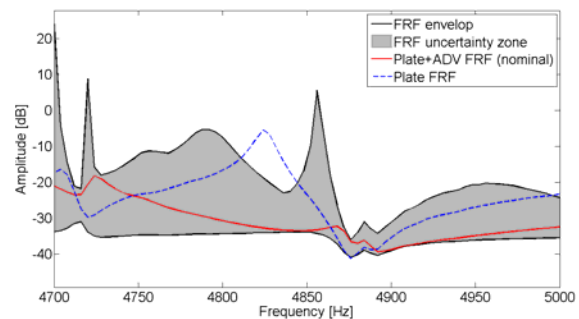
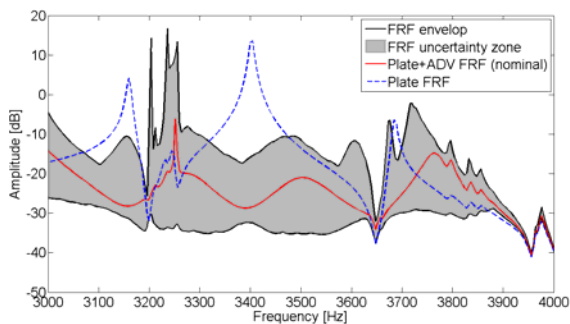


Figure 16 – FRF envelop of the system compressor + DVA after uncertainty propagation.

## 5. CONCLUSIONS

A methodology for optimal design of a multimodal dynamic vibration absorber was described in this paper. In the optimization, numerical evaluations of the DVA's natural frequencies were made with FEM composed with beams and point masses; this model predicts satisfactorily the response of the system with little computational effort and can be advantageously coupled with the experimental FRFs of the real primary system, by using a very efficient coupling procedure based on FRFs (either experimental or numerical) of the subsystems. Uncertainty propagation was also performed to evaluate the robustness of the system with respect to randomness which is inevitably present in real-world designs. The main interest is to evaluate the influence of geometrical variations on the attenuation performance of the DVA. The results obtained from Monte Carlo simulations demonstrate that such influence vary according to the target mode and indicate the necessity of performing the optimal design of the DVA in the framework of robust optimization techniques. Such development is currently conducted by the authors.

## 6. ACKNOWLEDGEMENTS

The authors gratefully acknowledge:

- The Brazilian Research Council – CNPq, for the continued support to their research work, especially through projects 484498/2007-0 and 310524/2006-7.
- Minas Gerais State Research Agency FAPEMIG, for the grant of a post-doctoral scholarship to Dr. E. Pillet
- CAPES Foundation, of the Brazilian Ministry of Education for the grant of a M.Sc. scholarship to Mr. Murilo B. Barros
- EMBRACO S.A. for partial funding of the research activities described in this paper.

## 7. REFERENCES

- Adhikari, S. and Friswell, M. I. and Lonkar, K. and Sarkar, A., 2009, "Experimental case studies for uncertainty quantification in structural dynamics", *Probabilistic Engineering Mechanics*, vol. 24, n°4, pp. 473-492.
- Blevins, R. D., 2001, "Formulas For Natural Frequency And Mode Shape", 4th Edition. Krieger Publishing Company.
- Brock, J. E., 1946, "A Note on the Damped Vibration Absorber", *Trans. A.S.M.E.*, A284.
- Crowley, J. R., Rochlin, G. T., Klosterman, A. L., Vold, H., 1984, "Direct Structural Modifications Using Frequency Response Functions", 2<sup>nd</sup> International Modal Analysis Conference, pp. 58-65.
- Cunha Jr. S. S., 1999, "Estudo Teórico e Numérico de Absorvedores Dinâmicos de Vibrações", Master's degree thesis, UFU, Uberlândia, MG.
- Den Hartog, J. P., 1956, "Mechanical Vibrations", 4th edition. McGraw-Hill, New York.
- Dessombz, O. and Thouverez, F. and Laîné, J. -P. and Jézéquel, L., 2001, "Analysis of mechanical systems using interval computations applied to finite element methods", *Journal of Sound and Vibration*, vol. 239, n°5, pp. 949-968.
- Dimarogonas, A., 1996, "Vibration for Engineers", 2nd edition, Prentice Hall.
- Jones, R. T., Pretlove, A. J., Eyre, R., 1981, "Two Cases Studies in the Use of Tuned Vibration Absorbers on Footbridges", *The Structural Engineering*, vol. 59B, n°2, pp. 27-32.
- Frahm, H., 1911, "Device for Damping Vibrations of Bodies", US Patent 989, 958.
- Helton, J. C. and Davis, F. J., 2003, "Latin hypercube sampling and the propagation of uncertainty in analyses of complex systems", *Reliability Engineering and System Safety*, vol. 81, n°5, pp. 23-69.
- Luft, R. W., 1979, "Optimal Tuned Mass Dampers for Buildings", *Journal of the Structural Division, Proceedings of the ASCE*, vol. 105, n° ST12, pp. 2766-2722.
- Massa, F. and Ruffin, K. and Tison, T. and Lallemand, B., 2008, "A complete method for efficient fuzzy modal analysis", *Journal of Sound and Vibration*, vol. 39, n°1-2, pp. 63-85.
- Nessler, G. I., Brown, D. L., Stouffer, D. C., Maddox, K. C., 1977, "Design of a Viscoelastic Dynamic Absorber for Machine Tool Applications", *Journal of Engineering for Industry, Transactions of the ASME*, paper n°76-WA, pp. 620-623.
- Oberkampf, W. L. and Deland, S. M. and Rutherford, B. M. and Diegert, K. V. and Alvin, K. F., 2002, "Error and uncertainty in modeling and simulation", *Reliability Engineering and System Safety*, vol. 75, n°3, pp. 333-357.
- Otte, D., Grangier, H., Leuridian, J. and Aquilina, R., 1991, "Prediction of the Dynamics of Structural Assemblies Using Measured FRF-Data: Some Improved Data Enhancement Techniques", *Proceedings of the International Modal Analysis Conference, USA*, pp. 909-917.
- Rade, D. A. and Steffen Jr., V., 1999, "Optimization of Dynamic Vibration Absorbers Over a Frequency Band", *Proceedings of the 17th International Modal Analysis Conference, Kissimmee, FL*, pp. 188-193.
- Ram, Y.M., Elhay, S., 1996, "The theory of a Multi-Degree-of-Freedom Dynamic Absorber", *Journal of Sound and Vibration*, vol. 195, n°4, pp. 607-615.
- Schüeller, G. I., 1997, "A state-of-the-art report on computational stochastic mechanics", *Probabilistic Engineering Mechanics*, vol. 12, n°4, pp. 197-321.
- Snowdon, J. C., Nobile, M. A., 1980, "Beamlike Dynamic Vibration Absorbers", *Acoustic*, vol. 44, pp. 98-108.
- Sudret, B., 2007, "Uncertainty propagation and sensitivity analysis in mechanical models -- Contributions to structural reliability and stochastic spectral methods", *Habilitation à diriger des recherches, Université Blaise Pascal, Clermont-Ferrand, France*.
- Sun, J. Q., Jolly, M. R., Norris, M. A., 1995, "Passive, Adaptive and Active Tuned Vibration Absorbers – A Survey", *Transactions of the ASME*, vol. 117, pp. 234-242.
- Teodoro, E. B., 1994, "Dynamics of a Power Line When Supported by a Compliant Energy Absorbers", Ph. D. Thesis, ISU.
- Worden, K. and Manson, G. and Lord, T. M. and Friswell, M. I., 2005, "Some observations on uncertainty propagation through a simple nonlinear system", *Journal of Sound and Vibration*, vol. 288, n°3, pp. 601-621.

## 8. RESPONSIBILITY NOTICE

The authors are the only responsible for the printed material included in this paper.